Original paper

Folia Neuropathologica

Identification of a miRNA biomarker for the large artery atherosclerosis subtype of acute ischemic stroke

Bo Zhou[1*], Bo Li[2*], Pin Feng[3*], Xin Wang[4], He Gao[4], Lifang Xu[4], Tianyi Wang[5], Xiaoling Guo[1]

[1]Department of Neurology, The 981st Hospital of the Chinese People's Liberation Army, Chengde, China, [2]Department of Orthopaedics, Sun Yat-Sen Memorial Hospital of Sun Yat-Sen University, Guangzhou, China, [3]Department of General Surgery, The 981st Hospital of the Chinese People's Liberation Army, Chengde, China, [4]Chengde Medical University, Chengde, Hebei Province, China, [5]Department of Orthopaedics, The 981st Hospital of the Chinese People's Liberation Army, Chengde, China

*These authors contributed equally to this study.

Folia Neuropathol 2022; 60 (2): 210-220 *DOI: https://doi.org/10.5114/fn.2022.117248*

Abstract

Aim of the study: *To identify miRNA biomarkers of arterial atherosclerosis subtypes in acute ischemic stroke.*
Material and methods: *40 participants recruited in our hospital from October 2017 to January 2018. There were 12 patients with acute ischemic stroke (AIS), 13 patients with atherosclerosis (AS) and 15 healthy subjects. They were divided into the AIS group, AS group and healthy control (HC) group. The miRNA expression levels of the AIS group, AS group and HC group were measured by miRNA microarray. Bioinformatics analysis was performed using the miRNA target prediction database.*
Results: *The expression of 3 miRNAs, miR-129-1-3p, miR-4312, miR-5196-3p, was significantly different between the AIS and AS/HC groups. Genes targeted by miR-129-1-3p were involved in 12 pathways, of which axon guidance, retrograde endocannabinoid signalling and sphingolipid signalling pathways were associated with axonal and synaptic function. miR-129-1-3p mimics significantly decreased cortical neurite length and Runx2 levels, while miR-129-1-3p inhibitors promoted neurite growth and increased Runx2 expression.*
Conclusions: *miR-129-1-3p may be a relevant biomarker for the diagnosis of stroke caused by large artery atherosclerosis and could represent a novel therapeutic target for stroke treatment.*

Key words: *stroke, artery atherosclerosis, MiRNA, microarray analysis, runt-related transcription factor.*

Introduction

Stroke is the second leading cause of death in the world [10]. Acute ischemic stroke is a disorder of blood supply to brain tissue caused by many reasons. It belongs to the most common type of stroke in clinic, accounting for 85% of stroke cases [16]. The disease has the characteristics of a high incidence rate, mortality, recurrence rate and high disability rate, which poses a major threat to patients' health and life. According to risk factors, clinical characteristics and diagnostic indicators, ischemic stroke can be divided into five types: large artery atherosclerosis (LAA), cardioembolism (CE), small artery

Communicating authors:
Xiaoling Guo, Department of Neurology, The 981st Hospital of the Chinese People's Liberation Army, No. 3, Puning Temple, Puning Road, Shuangqiao District, Chengde 067000, China, phone: +8603145980621, fax: +8603145980621; Tianyi Wang, Department of General Surgery, The 981st Hospital of the Chinese People's Liberation Army, No. 3, Puning Temple, Puning Road, Shuangqiao District, Chengde 067000, China, phone: +8603142160466, fax: +8603142160466, e-mail: tianyiwang1478@163.com

occlusion (SAO), stroke of other determined cause (SOC), and stroke of undetermined cause (SUC) [4].

MicroRNA (miRNA) is a kind of small non coding RNA that regulates gene expression by specifically binding to complementary RNA sequences [13]. MiRNA participates in the regulation of endothelial function and the degradation of extracellular matrix, affects the formation and rupture of atherosclerotic plaque, and promotes the proliferation and degradation of neurons and glial cells [8,14,15,22,23]. For example, miR-145 is associated with elevated levels of tissue factor (TF) in patients with venous thrombosis. In addition, the stimulation of miR-145 *in vivo* reversed the decline of miR-145 and reduced the level and activity of TF in thrombosis [21]. Another study showed that microbubbles can regulate PI3K/Akt/eNOS pathway by transmitting miR-125-a-5p [17], so as to enhance the survival and angiogenesis of endothelial cells. MiR-129-1-3p inhibits vascular endothelial growth factor (VEGF) through Runx2, inhibits the differentiation and angiogenesis of endothelial progenitor cells, and may participate in the high expression of miR-4312 in breast cancer cells. It may promote cell proliferation and inhibit cell apoptosis through targeting PDCD4.

This study aims to identify early diagnostic markers of stroke, discover potential pathophysiological processes, and provide new therapeutic targets for stroke through bioinformatics analysis and target gene verification.

Material and methods

Research object

From October 2017 to January 2018, we recruited a total of 40 participants from the hospital. A total of 12 acute ischemic stroke (AIS) patients, 13 atherosclerosis (AS) patients and 15 healthy subjects were included in the study. All participants provided written informed consent. This study was approved by the ethics committee of our hospital.

Inclusion criteria: 1) ischemic stroke symptoms occurred within 6 hours; 2) all the patients included were stroke of large-artery atherosclerosis (LAA) subtype, which met the diagnostic criteria of cerebral infarction in the 2018 China guidelines for the diagnosis and treatment of acute ischemic stroke [9]; 3) TOAST classification was confirmed as large atherosclerotic cerebral infarction by magnetic resonance angiography or computed tomography angiography (CTA) [7]; 4) the onset time was less than 2 weeks; 5) patients with the first acute ischemic stroke; 6) complete at least one cranial vascular examination during hospitalization, including magnetic resonance angiography (MRA), CTA or digital subtraction angiography (DSA).

Exclusion criteria: 1) neuroimaging showed cerebral haemorrhage or brain dysfunction caused by other non-vascular causes (such as brain tumour, brain metastasis, subdural hematoma, epilepsy, brain trauma, etc.); 2) transient ischemic attack; 3) limb motor or sensory dysfunction caused by other diseases; 4) those who have taken contraindicated drugs; 5) rejected participants.

According to NASCET criteria, 13 patients with carotid stenosis of more than 50% were prospectively included in the group of large atherosclerosis with transient ischemic attack (TIA) (AS). The healthy control group (HC) refers to healthy adults of the same age group, without the history of stroke and major atherosclerosis. All subjects had past vascular risk factors, such as hypertension, hyperlipidaemia, diabetes and smoking, all examined by the same neuroscientist.

Research method

Collection and processing of blood samples

Blood samples were taken from patients with AIS within 6 hours after the onset of symptoms, and routine blood samples were taken for AS and HC groups. All blood samples were placed in tubes containing EDTA (BD Bioscience). Plasma was separated after differential centrifugation (2000 g for 10 minutes, 2500 g for 15 minutes, 15°C). Plasma samples were carefully collected and put into RNase free EP tube, and stored at –80°C for standby.

RNA isolation

Total RNA was isolated from the plasma samples using the mirVana™ PARIS™ Kit9 (Ambion, Texas, USA). The concentration of RNA samples was quantified using the Nanodrop ND-2000 (Thermo Scientific, Wilmington, DE, USA) and RNA integrity was determined using the Agilent 2100 bioanalyzer (Agilent Technologies, Palo Alto, CA).

MiRNA microarray analysis and target gene prediction

miRNAs were detected using the Agilent miRNA microarray platform (Stanley Medical Research Insti-

tute Online Genomics Database). Total RNA (100 ng) was dephosphorylated, denatured, and the 3' end of the RNA was labelled with Cyanine-3-CTP (Cy3). The marked RNA was purified and hybridized on microRNA arrays in a hybridization oven (Agilent Technologies, Palo Alto, CA). The chips were scanned with the Agilent G2505C microarray scanner. Raw data were extracted from the original images using the Feature Extraction software (version 10.7.1.1, Agilent Technologies) and then normalized and analysed using the GeneSpring software (version 13.1, Agilent Technologies). miRNA differential expression analysis was performed using a *t* test. Up- or down-regulation with a ≥ 2 fold change and a p value ≤ 0.05 was considered statistically significant. Three databases, including TargetScan V7.1 (http://targetscan.org/), miRwalk V2.0 (http://mirwalk.umm.uni-heidelberg.de/) and miRDB (http://mirdb.org/miRDB/) were used to predict miRNA target genes. Four databases (miRBD, miRWalk, Starbase v2.0 (http://starbase.sysu.edu.cn/index.php) and TargetScan) were used to predict the potential miRNAs targeting Runx2.

Protein-protein interaction network and functional enrichment

STRING V11.0 (http://string.embl.de/) was used to identify the protein-protein interaction (PPI) of targets of the differentially expressed miRNA. PPIs were then visualized using Cytoscape software v3.2.1 (https://github.com/nolanlab/cytospade). Gene ontology (GO) and KEGG analysis were conducted using DAVID (http://david.abcc.ncifcrf.gov/) to identify gene ontology annotation of the target genes.

Cortical neuronal culture

To verify the regulatory role of miR-129-1-3p in axonal outgrowth, cortical neurons from adult Wistar Rats were extracted as previously reported [24]. In brief, the cortical tissues were extracted from the brain and cut into pieces. Then, the cortical tissue was digested to a single cell suspension with 0.125% Trypsin. The DMEM (10% fetal bovine serum [FBS]) was subsequently used to stop the digestion. Single cortical neurons were seeded into poly-L-Lysine-coated 24- or 6-well plates for immunofluorescence staining and western blotting.

Transfection

To confirm the regulatory role of miR-129-1-3p on the axonal outgrowth of cortical neurons, miR-129-1-3p mimics, inhibitors, or negative control sequences were transfected into cultured cortical neurons with Lipofectamine 2000 (Invitrogen, USA). The transfected efficiency was determined with transfecting FITC-oligo and was 85-95%. At 24 hours post transfection, the cell cultured medium was changed to normal culture medium.

Immunofluorescence staining

The cultured cortical neurons were washed with phosphate buffered saline (PBS), fixed with 4% paraformaldehyde, incubated with 10% blocking buffer and probed with primary (NF-200) and secondary (anti-rabbit-FITC) antibodies. Images were acquired using a Fluorescence microscope (Nikon TiU, Tokyo, Japan) and neurite length was manually quantified using the Image-Pro Plus 6.0 software (Media Cybernetics, Silver Spring, MD, USA).

Western blot

Cultured neurons were harvested and the total protein was extracted using RIPA buffer (Santa Cruz, Dallas, USA). Samples were treated with protease inhibitor to prevent degradation. After concentration determination on the Nanodrop ND-2000 (ThermoScientific, Wilmington, DE, USA), proteins were separated using SDS-PAGE electrophoresis and transferred onto a membrane. Anti-Runx2 antibody and anti-rabbit-HRP were applied to determine the relative expression of Runx2. The relative expression of Runx2 was normalized against the expression of GAPDH. Experiments were repeated at least three times.

Statistical analysis

All experiments were statistically analysed by statistical analysis system software SPSS 21.0 (Chicago, Illinois, USA). Data conforming to normal distribution are expressed as mean ± standard deviation. *T*-test was used to test the significant difference. The Kolmogorov-Smirnov (K-S) test was used to test the normality of the data. The measured data showed a non-normal distribution, so it was expressed in the median (quartile), and the Mann-Whitney *U* test was used for inter-group comparison. $P < 0.05$ was considered statistically significant.

Results

Comparison of baseline data of patients with HC, AS and AIS

Among the 12 patients in the AIS group, there were 6 males and 6 females, with an average age of

64 ±3.40 years. There were 4 males and 9 females in the AS group, with an average age of 68.77 ±3.40 years. Among the 15 patients in the HC group, there were 5 males and 10 females, with an average age of 65.47 ±0.72. There was no significant difference in other baseline data ($p > 0.05$), which were comparable (see Table I).

Comparison of miRNA expression among HC, AS and AIS groups

There were significant differences in 27 miRNAs between the AIS group and the HC group (Fig. 1A, Table II), while there were differences in 9 miRNAs between the AIS group and the AS group (Fig. 1B, Table III). There were differences in the expression of three miRNAs (miR-129-1-3p, miR-4312, miR-5196-3p) in the AIS group compared with HC and AS groups (Fig. 1C).

To compare the expression of three different miRNAs in these groups, we used the standardized total probe signal of miRNA microarray. miR-129-1-3p and miR-4312 were highly expressed in the AS group and further increased in the AIS group, while the expression of miR-5196-3p decreased slightly in the AS group but increased in the AIS group (Fig. 1D). These results suggest that miR-129-1-3p and miR-4312 may be involved in the pathophysiology of AIS.

Bioinformatics analysis of miR-129-1-3p

In order to study the pathophysiological process and molecular mechanism of differentially expressed miRNA, focusing on miR-129-1-3p, miRNA target prediction databases (TargetScan, miRWalk and miRDB) were used for bioinformatics analysis. The analysis identified 172 target genes of miR-129-1-3p. To elucidate the protein interactions of these target genes, string analysis was applied and the results were visualized using Cytoscape (Fig. 2A). In this protein-protein interaction network, Runx2 is the key target gene of miR-129-1-3p, which is widely associated with other proteins.

Biological effect analysis of miR-129-1-3p

To further elucidate the possible biological effects of miR-129-1-3p, GO and KEGG pathways were analysed using David database. The enrichment biological process of miR-129-1-3p and its target was analysed (Fig. 2B-E). Mir-129-1-3p and its targets are involved in 19 biological processes (Fig. 2B), including the regulation of calcineurin NFAT signal cascade, positive regulation of calcium dependent exocytosis, regulation of sodium transmembrane transporter activity, calcium regulated neurotransmitter exocytosis and axon guidance. Cell composition analysis showed that the presynaptic active region, voltage-gated calcium channel complex, synapse, axon and postsynaptic membrane were enriched (Fig. 2C). In terms of molecular function, transcription factor activity, sodium channel regulator activity and ion channel binding were enhanced (Fig. 2D). KEGG analysis showed that the target of miR-129-1-3p was enriched in axon guidance, retrograde endogenous cannabinoid signal, sphingolipid signal pathway and other 9 pathways (Fig. 2E). These results suggest that miR-129-1-3p may regulate the function of neurites and synapses.

The regulatory role of miR-129-1-3p in cortical neurite outgrowth

Mir-129-1-3p was interfered in cultured cortical neurons to confirm the interaction between miR-129-1-3p and Runx2. Mir-129-1-3p simulant inhibited cortical axon growth, while miR-129-1-3p inhibitor promoted cortical neuron axon growth ($p < 0.05$)

Table I. The demographic characteristics and vascular risk factors were compared among acute ischemic stroke, atherosclerosis and healthy controls groups

Characteristics	HC	AS	AIS
Age	65.47 ±0.72	68.77 ±3.40	64 ±3.40
Hypertension	0 (0%)	13 (92.9%)	7 (53.8%)
Diabetes	0 (0%)	3 (21.4%)	6 (50%)
Smoking	4 (26.7%)	5 (35.7%)	6 (50%)
TC	0.78 ±0.06	1.54 ±0.18	1.34 ±0.14
HDL	2.23 ±0.09	2.8 ±0.24	3.38 ±0.34
LDL	1.33 ±0.06	1.12 ±0.54	1.36 ±0.09
PLT	204 ±6.21	189 ±7.64	235.42 ±19.48
ApoA1	2.09 ±0.41	1.20 ±0.05	1.44 ±0.09
ApoB	0.93 ±0.03	0.81 ±0.05	0.97 ±0.85
CRP	1.44 ±0.03	5.86 ±1.47	6.06 ±1.37

AIS – acute ischemic stroke, AS – atherosclerosis, HC – healthy control subjects, SD – standard deviation, LDL – low-density lipoprotein, HDL – high-density lipoprotein, TC – total cholesterol, PLT – platelets, ApoA1 – apolipoprotein A-1, ApoB – apolipoprotein B, CRP – C-reactive protein

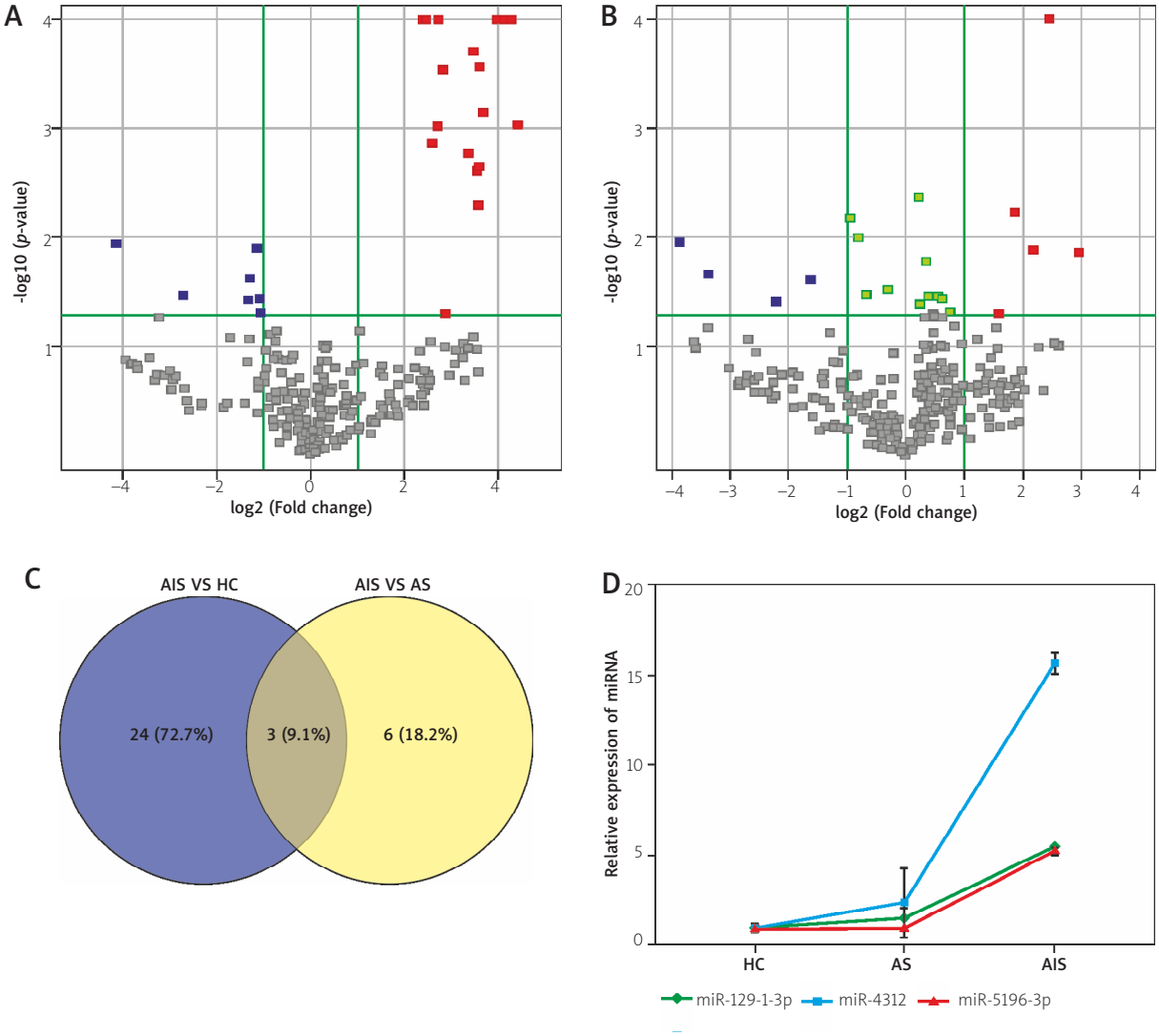

Fig. 1. Differential expression of miRNAs among HC, AS and AIS groups. **A**) Volcano Plot of differential expression miRNAs between AIS and HC group. **B**) Volcano Plot of differential expression miRNAs between AIS and AS groups (Log2Fold changes > 1, $p < 0.05$). Red blocks indicate elevated differentially expressed miRNAs; green blocks indicate reduced differentially expressed miRNAs; grey blocks indicate miRNAs with no expression difference. **C**) miRNA differential expression between HC, AS, and AIS groups in a Venn diagram. The Venn diagram shows that three miRNAs (miR-129-1-3p, miR-4312, miR-5196-3p) were differentially expressed in the AIS group compared to HC and AS groups. **D**) The expression levels of miR-129-1-3p, miR-4312, miR-5196-3p in HC, AS and AIS groups. miR-129-1-3p and miR-4312 were highly expressed in the AS group and further increased in the AIS group. The expression of miR-5196-3p was decreased slightly in the AS group, but was elevated in the AIS group.

(Fig. 3B, C). Similarly, miR-129-1-3p simulation significantly down regulated Runx2 levels, while miR-129-1-3p inhibitors promoted Runx2 expression ($p < 0.05$) (Fig. 3D, E). These results suggest that miR-129-1-3p has a negative effect on the growth of cortical axons by targeting Runx2.

Discussion

Acute ischemic stroke has a high incidence and mortality rate and is a serious global medical issue. Accurate and rapid identification of AIS plays an important role in shortening the time before blood flow

Table II. List of differentially expressed miRNAs in acute ischemic stroke

miRNAs	*P* value	Regulation	Fold change
miR-1273f	0.033371855	Down	6.458823
miR-1299	0.011499343	Down	17.777027
miR-3663-3p	0.036396313	Down	2.1093192
miR-4323	0.012690264	Down	2.1887002
miR-6087	0.023496168	Down	2.4054167
miR-6870-3p	0.049042206	Down	2.0777457
miR-765	0.03796658	Down	2.5112484
miR-129-1-3p	1.95E-07	Up	5.471257
miR-129-2-3p	0.00140898	Up	6.078157
miR-296-5p	0.002465383	Up	11.582435
miR-3151-3p	0.002273256	Up	11.992406
miR-3620-3p	0.04907799	Up	7.42919
miR-4312	9.59E-08	Up	15.551289
miR-4646-3p	2.01E-04	Up	11.134249
miR-4666b	5.90E-05	Up	17.304768
miR-4701-5p	3.04E-05	Up	19.272366
miR-5010-3p	7.30E-04	Up	12.716985
miR-5196-3p	3.05E-07	Up	5.2247877
miR-6756-3p	0.005132715	Up	11.8222885
miR-6759-3p	2.06E-05	Up	18.900421
miR-6796-3p	0.001725446	Up	10.2778015
miR-6834-3p	9.64E-04	Up	6.544613
miR-6855-3p	3.97E-05	Up	19.149551
miR-6877-3p	9.20E-04	Up	21.026161
miR-7114-3p	2.92E-04	Up	7.135053
miR-7845-5p	4.56E-05	Up	6.6251874
miR-98-3p	2.73E-04	Up	12.1707945

Table III. List of differentially expressed miRNAs between acute ischemic stroke and atherosclerosis groups

miRNAs	*P* value	Regulation	Fold change
miR-184	0.01112759	Down	14.416237
miR-21-5p	0.02421851	Down	3.0550556
miR-29a-3p	0.03817539	Down	4.585285
miR-6774-5p	0.02157482	Down	10.382845
miR-129-1-3p	0.00594998	Up	3.6751456
miR-223-3p	0.04951954	Up	3.0386822
miR-4312	0.01372297	Up	7.9141707
miR-5196-3p	3.38E-08	Up	5.554728
miR-6890-3p	0.01293834	Up	4.6251683

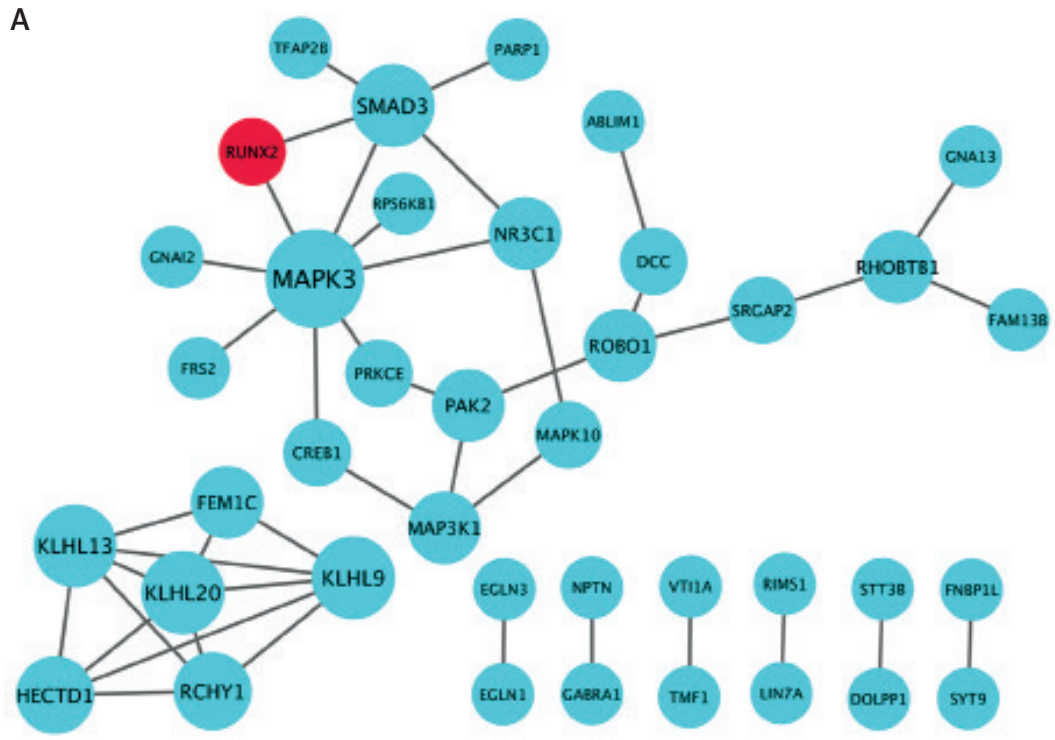
A
TFAP2B
PARP1
SMAD3
RUNX2
ABLIM1
GNA13
RPS6KB1
NR3C1
GNAI2
MAPK3
DCC
RHOBTB1
SRGAP2
FAM13B
ROBO1
FRS2
PRKCE
PAK2
MAPK10
CREB1
FEM1C
MAP3K1
KLHL13
KLHL20
KLHL9
EGLN3
NPTN
VTI1A
RIMS1
STT3B
FNBP1L
HECTD1
RCHY1
EGLN1
GABRA1
TMF1
LIN7A
DOLPP1
SYT9

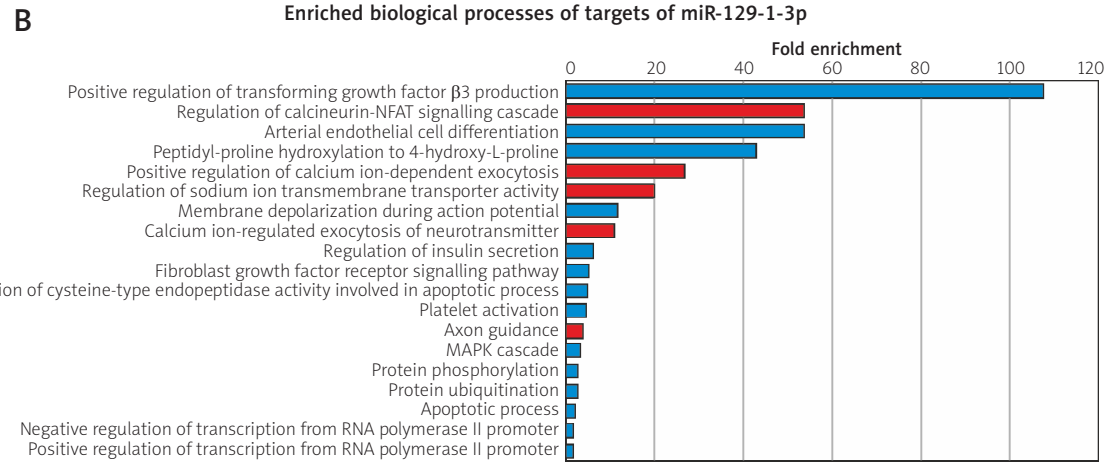
B
Enriched biological processes of targets of miR-129-1-3p
Fold enrichment
0
20
40
60
80
100
120
Positive regulation of transforming growth factor β3 production
Regulation of calcineurin-NFAT signalling cascade
Arterial endothelial cell differentiation
Peptidyl-proline hydroxylation to 4-hydroxy-L-proline
Positive regulation of calcium ion-dependent exocytosis
Regulation of sodium ion transmembrane transporter activity
Membrane depolarization during action potential
Calcium ion-regulated exocytosis of neurotransmitter
Regulation of insulin secretion
Fibroblast growth factor receptor signalling pathway
Activation of cysteine-type endopeptidase activity involved in apoptotic process
Platelet activation
Axon guidance
MAPK cascade
Protein phosphorylation
Protein ubiquitination
Apoptotic process
Negative regulation of transcription from RNA polymerase II promoter
Positive regulation of transcription from RNA polymerase II promoter

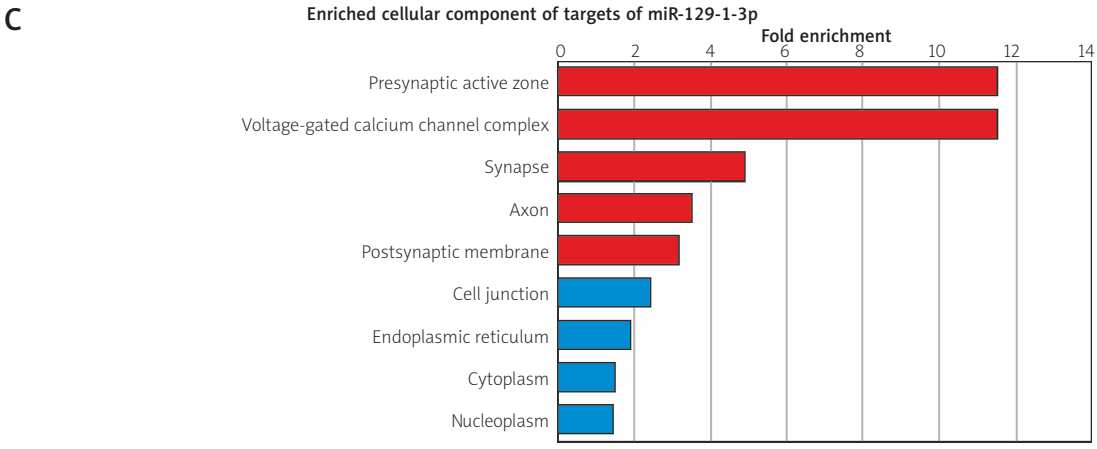
C
Enriched cellular component of targets of miR-129-1-3p
Fold enrichment
0
2
4
6
8
10
12
14
Presynaptic active zone
Voltage-gated calcium channel complex
Synapse
Axon
Postsynaptic membrane
Cell junction
Endoplasmic reticulum
Cytoplasm
Nucleoplasm

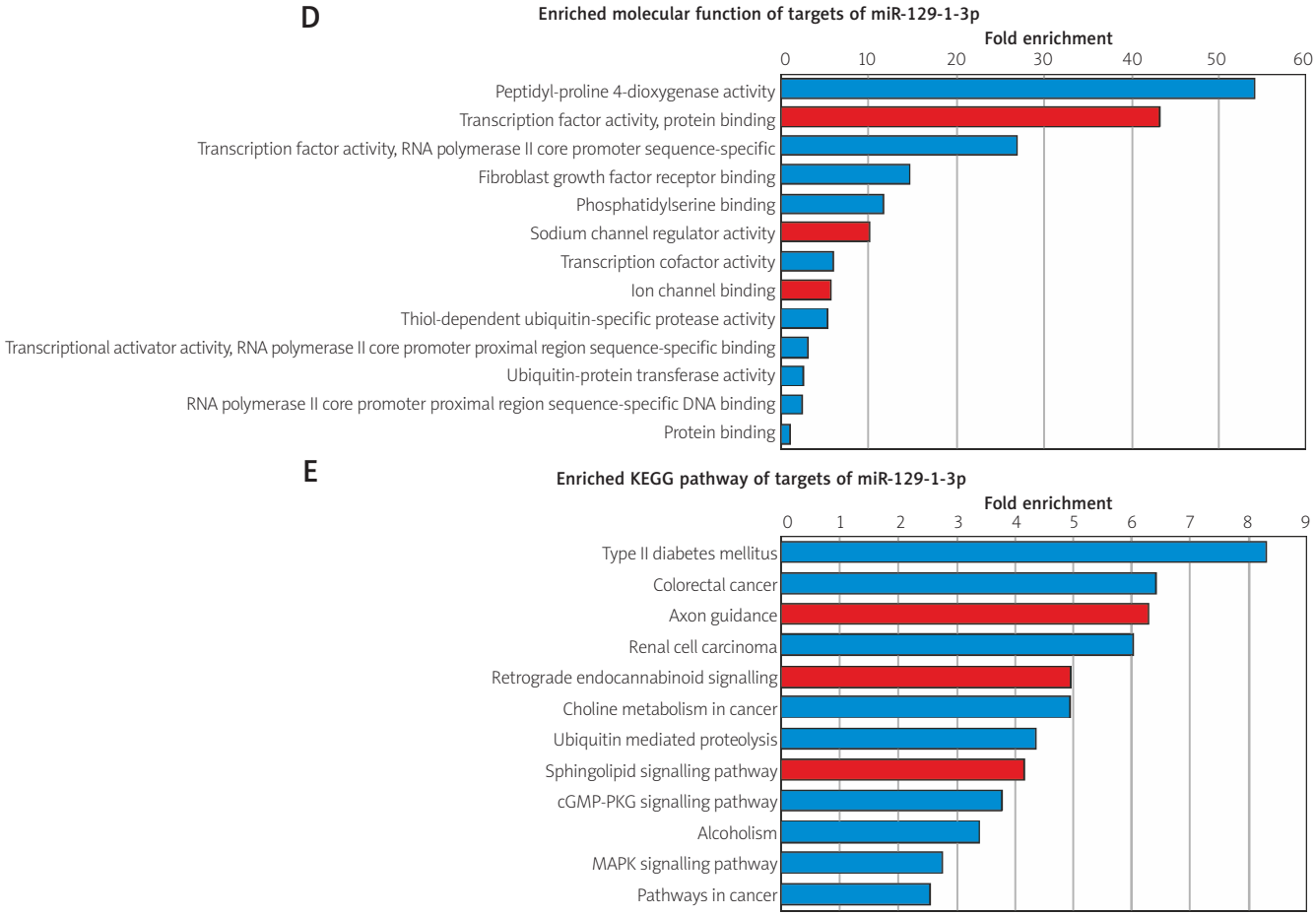

Fig. 2. Biological function of miR-129-1-3p target genes. **A**) The protein interaction network of miR-129-1-3p. Active interaction sources included text mining, experiments, database, and co-expression. Runx2 is widely associated with other proteins in the protein interaction network of miR-129-1-3p target genes. **B-E**) GO Enrichment and KEGG pathway analysis of miR-129-1-3p target genes. The height of each histogram indicated the fold enrichment for the corresponding cellular component. Red histogram bars are related to neurite growth and synaptic function.

to the brain is restored and therefore can affect prognosis. Our study investigated potential biomarkers and treatment targets for LAA-type AIS, which was the one of AIS hypotypes rarely research by current study.

In our study, we compared plasma miRNAs expression levels in a patient group with LAA subtypes of acute ischemic stroke (AIS), stroke-free large arteriosclerosis (AS) and healthy controls using microarray analysis. MiR-129-1-3p, miR-4312 and miR-5196-3p were differentially expressed in the AIS group compared with AS and HC groups; miR-129-1-3p and miR-4312 were upregulated in both AS and AIS groups. A recent review concluded that more than twenty miRNAs were differentially expressed in the AIS group, such as miR-106b was reported as differentially expressed in at least 2 studies [20]. However, to our knowledge, this is the first study to show a differential expression of miR-129-1-3p and mir-4312 in both AIS and AS groups. Thus, we selected miR-129-1-3p to further explore its possible biological function and investigate its target genes in relation to AIS.

Gene ontology (GO) and KEGG pathway analysis revealed that target genes of miR-129-1-3p were enriched in pathways associated with axonal and synaptic regulation, including axon guidance, retrograde endocannabinoid signalling and the sphingolipid signalling pathway [1,3,20]. The axon guidance pathway has also been shown to been rich in AIS in another study [12], it suggests that axon growth plays an important role in the pathological process of AIS. Furthermore, the current researches focus on identifying the differentially expressed microRNAs profiles of yang and yin syndromes in the AIS patient, aim to provide the different molecular basis of the different

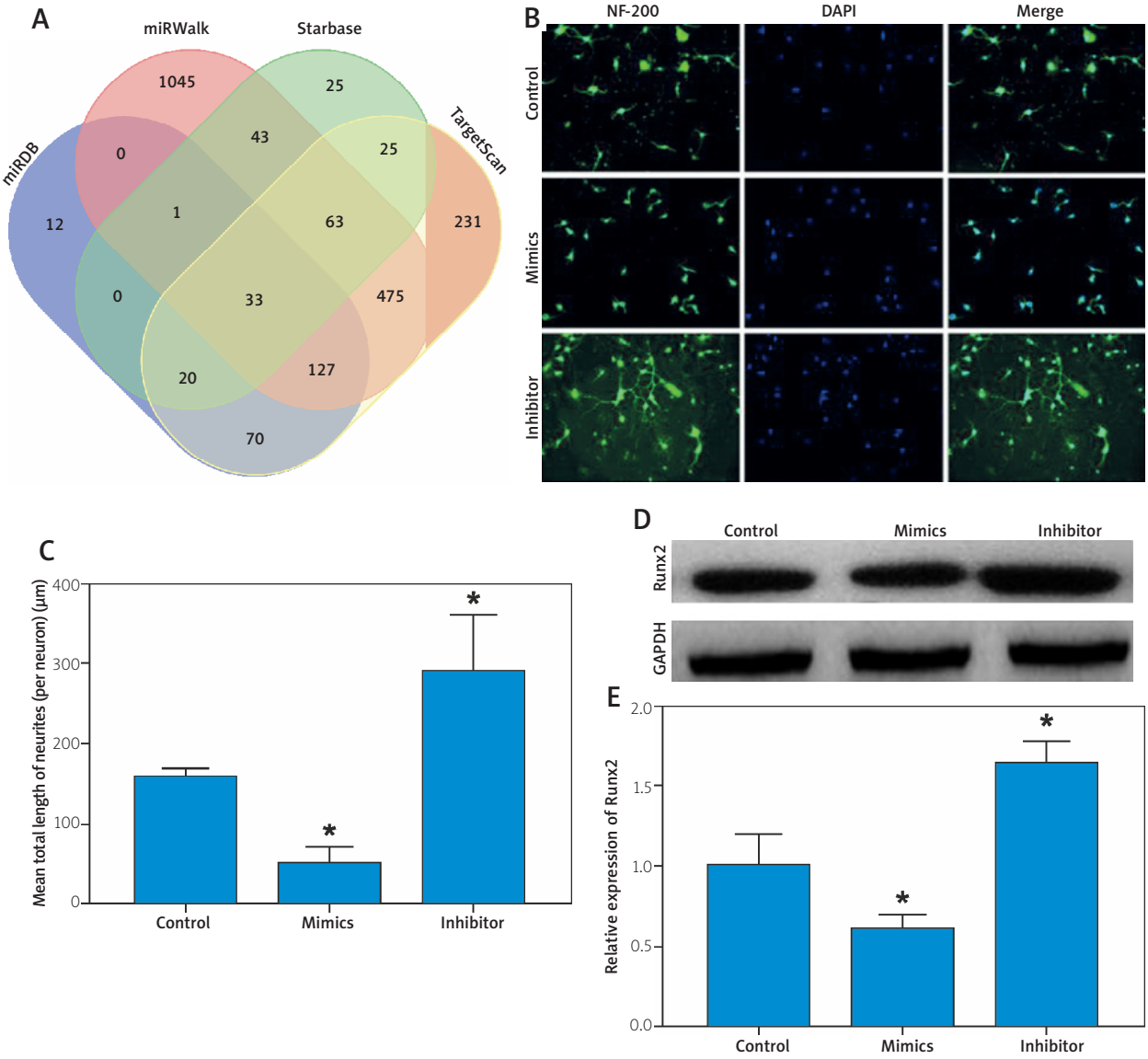

Fig. 3. The regulatory role of miR-129-1-3p in cortical neurite outgrowth. **A**) Potential miRNAs targeting Runx2 from four databases. All four databases return miR-129-1-3p. **B, C**) Neuronal outgrowth in presence of miR-129-3p mimics and inhibitor. miR-129-3p mimics inhibited the cortical neuron axon growth while miR-129-3p inhibitor enhanced the cortical neuron axon growth. **D, E**) Mir-129-3p negatively regulates Runx2. miR-129-3p mimics significantly downregulated level of Runx2, while miR-129-3p inhibitor promoted the expression of Runx2.

classification. For example, Zhao *et al*. reported that the key regulatory miRNAs, gene, and pathways in the yang syndrome were hsa-miR-93-5p and -320b, enabled homolog, the metabolic pathways and mitogen-activated protein kinase signalling pathways, respectively, while those in the yin syndrome were hsa-miR-424-5p and -106b-5p, CNOT4, hepatitis B and pathways in cancer, respectively [25].

Our database analysis predicted that Runx2 might be a target gene of miR-129-1-3p. The current study has demonstrated that miR-129-1-3p could target Runx2 in endothelial progenitor cells and thus to inhibit endothelial progenitor cell differentiation and angiogenesis [11]. However, no studies have so far been conducted to verify the interaction of miR-129-1-3p and Runx2 in cortical neurons. In the central nervous system, Runx2 is expressed in the suprachiasmatic nucleus, paraventricular nucleus, and olfactory bulb [19]. Following SNC injury, levels of Runx2 significantly increase within 3 days, peak after

1 week, and then return to normal levels by 4 weeks. When Runx2 expression is inhibited, neurite outgrowth in PC12 cells stimulated with NGF for 3 days can be inhibited, and a decrease in NF200 expression, which is closely related to neurite outgrowth, is observed [6]. Chen *et al*. have shown that Runx2 can reduce the inhibitory effect of high glucose-induced osteoblast differentiation by regulating the PI3K/AKT/GSK3β/β-catenin pathway [5]. And Bai *et al*. proposed that miR-196b can inactivate the PI3K/AKT/GSK3β pathway through the down-regulation of Runx2 [2]. The PI3K/Akt/GSK3β pathway is essential for neuronal differentiation [6]. In addition, PI3K is also related to the formation of autophagosomes, and an increase of autophagosomes is detected in brain tissue after stroke [18], suggesting that miR-129-1-3p may induce the loss of autophagocyte-related neurons, aggravating stroke injury by targeting the Runx2/PI3K pathway.

This study has some limitations. Firstly, the sample size included in the study was small, and the potential confounding factors such as lifestyle and family history were not controlled. Our results need to be further validated in larger studies to confirm the elevated level of miR-129-1-3p in large atherosclerosis in acute ischemic stroke. In addition, it is also necessary to determine the sensitivity and specificity of miR-129-1-3p in detecting LAA-AIS and its expression in other types of ischemic stroke.

Conclusions

In summary, our study suggests that miR-129-1-3p and miR-4312 may be involved in the pathophysiological process of AIS. It was also revealed that miR-129-1-3p targets Runx2 and affects axon growth in cortical neurons. Our results also suggest that miR-129-1-3p may be a biomarker of arterial cerebral infarction and may further represent a therapeutic target for stroke.

Ethics approval and consent to participate

This study was conducted in accordance with the Declaration of Helsinki. This study was conducted with the approval from the Ethics Committee of The 981st Hospital of the Chinese People's Liberation Army. After explaining the operation steps, all patients gave their informed consent.

Acknowledgments

The authors would like to thank all the reviewers who participated in the review and staff members in the 981st Hospital of the Chinese People's Liberation Army for continuous support.

Funding

This work was supported by the General Project of Hebei Natural Science Foundation [No. H2020406027, H2017101030].

Disclosure

The authors report no conflict of interest.

References

1. Araque A, Castillo PE, Manzoni OJ, Tonini R. Synaptic functions of endocannabinoid signaling in health and disease. Neuropharmacology 2017; 124: 13-24.
2. Bai X, Meng L, Sun H, Li Z, Zhang X, Hua S. MicroRNA-196b inhibits cell growth and metastasis of lung cancer cells by targeting Runx2. Cell Physiol Biochem 2017; 43: 757-767.
3. Chan JP, Sieburth D. Localized sphingolipid signaling at presynaptic terminals is regulated by calcium influx and promotes recruitment of priming factors. J Neurosci 2012; 32: 17909-17920.
4. Chen PH, Gao S, Wang YJ, Xu AD, Li YS, Wang D. Classifying Ischemic Stroke, from TOAST to CISS. CNS Neurosci Ther 2012; 18: 452-456.
5. Chen Y, Hu Y, Yang L, Zhou J, Tang Y, Zheng L, Qin P. Runx2 alleviates high glucose-suppressed osteogenic differentiation via PI3K/AKT/GSK3β/β-catenin pathway. Cell Biol Int 2017; 41: 822-832.
6. Ding D, Zhang P, Liu Y, Wang Y, Sun W, Yu Z, Cheng Z, Wang Y. Runx2 was correlated with neurite outgrowth and Schwann cell differentiation, migration after sciatic nerve crush. Neurochem Res 2018; 43: 2423-2434.
7. Gui X, Wang L, Wu C, Wang H, Kong J. Prognosis of subtypes of acute large artery atherosclerotic cerebral infarction by evaluation of established collateral circulation. J Stroke Cerebrovasc Dis 2020; 29: 105232.
8. Haemmig S, Feinberg MW. MicroRNAs as harbingers of high-risk carotid artery atherosclerotic disease? Circ Res 2017; 120: 596-598.
9. Huo XC, Gao F. Chinese guidelines for intravascular treatment of acute ischemic stroke 2018. Chinese J Stroke 2018; 13: 706-729.
10. Kuriakose D, Xiao Z. Pathophysiology and treatment of stroke: present status and future perspectives. Int J Mol Sci 2020; 21: 7609.
11. Li N, Wang WB, Bao H, Shi Q, Jiang ZL, Qi YX, Han Y. Micro-RNA-129-1-3p regulates cyclic stretch-induced endothelial progenitor cell differentiation by targeting Runx2. J Cell Biochem 2019; 120: 5256-5267.

12. Li P, Teng F, Gao F, Zhang M, Wu J, Zhang C. Identification of circulating microRNAs as potential biomarkers for detecting acute ischemic stroke. Cell Mol Neurobiol 2015; 35: 433-447.
13. Lu TX, Rothenberg ME. MicroRNA. J Allergy Clin Immunol 2018; 141: 1202-1207.
14. Lv J, Li S, Wan T, Yang Y, Cheng Y, Xue R. Inhibition of microRNA-30d attenuates the apoptosis and extracellular matrix degradation of degenerative human nucleus pulposus cells by up-regulating SOX9. Chem Biol Interact 2018; 296: 89-97.
15. Madelaine R, Sloan SA, Huber N, Notwell JH, Leung LC, Skariah G, Halluin C, Paşca SP, Bejerano G, Krasnow MA, Barres BA, Mourrain P. MicroRNA-9 couples brain neurogenesis and angiogenesis. Cell Rep 2017; 20: 1533-1542.
16. Mendelson SJ, Prabhakaran S. Diagnosis and management of transient ischemic attack and acute ischemic stroke: a review. JAMA 2021; 325: 1088-1098.
17. Pan Q, Ma C, Wang Y, Wang J, Zheng J, Du D, Liao X, Chen Y, Chen Y, Bihl J, Chen C, Yang Y, Ma X. Microvesicles-mediated communication between endothelial cells modulates, endothelial survival, and angiogenic function via transferring of miR-125a-5p. J Cell Biochem 2019; 120: 3160-3172.
18. Puyal J, Ginet V, Clarke PG. Multiple interacting cell death mechanisms in the mediation of excitotoxicity and ischemic brain damage: a challenge for neuroprotection. Prog Neurobiol 2013; 105: 24-48.
19. Reale ME, Webb IC, Wang X, Baltazar RM, Coolen LM, Lehman MN. The transcription factor Runx2 is under circadian control in the suprachiasmatic nucleus and functions in the control of rhythmic behavior. PLoS One 2013; 8: e54317.
20. Russell SA, Bashaw GJ. Axon guidance pathways and the control of gene expression. Dev Dyn 2018; 247: 571-580.
21. Sahu A, Jha PK, Prabhakar A, Singh HD, Gupta N, Chatterjee T, Tyagi T, Sharma S, Kumari B, Singh S, Nair V, Goel S, Ashraf MZ. MicroRNA-145 impedes thrombus formation via targeting tissue factor in venous thrombosis. EBioMedicine 2017; 26: 175-186.
22. Santulli G. MicroRNAs and endothelial (dys) function. J Cell Physiol 2016; 231: 1638-1644.
23. Saxena S, Jain A, Rani V. MicroRNA-mediated MMP Regulation: Current diagnostic and therapeutic strategies for metabolic syndrome. Curr Gene Ther 2017; 17: 214-227.
24. Wang Z, Yuan W, Li B, Chen X, Zhang Y, Chen C, Yu M, Xiu Y, Li W, Cao J, Wang X, Tao W, Guo X, Feng S, Wang T. PEITC promotes neurite growth in primary sensory neurons via the miR-17-5p/STAT3/GAP-43 axis. J Drug Target 2019; 27: 82-93.
25. Zhao HP, Liu P, Xu CM, Li GW, Gao L, Luo YM. Unique MicroRNAs signature of lymphocyte of Yang and Yin syndromes in acute ischemic stroke patients. Chin J Integr Med 2019; 25: 590-597.